Channel delineation and chert reservoir characterization by integrated seismic texture segmentation and cluster analysis

Marcilio Castro de Matos*[1,2], Malleswar (Moe) Yenugu[2] , Sipuikinene Miguel Angelo[3] and Kurt J. Marfurt[2]
[1]*Sismo Research&Consulting;* [2]*University of Oklahoma;* [3] *Statoil Norway*

This paper was prepared for presentation during the 12th International Congress of the Brazilian Geophysical Society held in Rio de Janeiro, Brazil, August 15-18, 2011.

Abstract

In recent years, 3D volumetric attributes have gained wide acceptance by seismic interpreters. The early introduction of single-trace complex trace attributes was quickly followed by seismic sequence attribute mapping workflows. 3D geometric attributes such as coherence and curvature are also widely used. Most of these attributes correspond to very simple, easy-to-understand measures of a waveform or surface morphology. However, not all geologic features can be so easily quantified. For this reason, simple statistical measures of the seismic waveform such as RMS amplitude and texture analysis techniques prove to be quite valuable in delineating more chaotic stratigraphy. In this paper, we coupled structure-oriented texture analysis based on the gray-level co-occurrence matrix with self-organizing maps clustering technology and applied it to classify seismic textures. By this way, we expect our workflow should be more sensitive to lateral changes rather than vertical changes in reflectivity. We applied the methodology to a 3D seismic survey acquired over OsageCo., OK, USA. and our results indicate that our method can be used to delineate the meandering channels as well as to characterize chert reservoirs.

Introduction

One of the main goals of reflection seismology is to analyze the seismic waveform and amplitude to predict lithologic facies, reservoir compartmentalization and rock properties such as porosity and thickness by analyzing the seismic waveform and amplitude. Seismic attribute analysis is a technique that is commonly used by the oil industry to delineate stratigraphic and structural features of interest. Seismic attributes are particularly important in allowing the interpreter to enhance and visualize subtle features. For example, coherence can generate easy-to-understand images of polygonally-faulted dewatered shales that may be difficult to see on seismic amplitude time slices. Curvature can enhance long wavelength flexures and folds in and out of the plane of visualization. Spectral components may highlight subtle thin bed tuning effects. Many commercial seismic interpretation packages contain schemes to calculate attributes such as RMS amplitude and relative impedance, both of which are sensitive to changes in acoustic impedance. Each of these attributes is based on a very simple geometric or physical model that can be related to structure, stratigraphy, diagenesis, or data quality.

Not all geologic features follow such a simple model. Experienced interpreters can easily recognize the seismic response of a crystalline basement, mass transport complexes, and carbonate reef buildups. However, when put to the task they find it difficult to quantitatively define how they do their interpretation. Such interpreters (and human beings in general) are experts at texture analysis. Our study focuses upon seismic texture analysis, borrowing techniques commonly used in remote sensing to map terrain, vegetation, and land-use information. Textures are frequently characterized as different patterns in the underlying data. Seismic texture analysis was first introduced by Love and Simaan (1984) to extract patterns of common seismic signal character. More recently, West et al. (2002), Gao, (2003, 2004, 2007, 2009), and Chopra and Alexeev (2006) have extended texture analysis to seismic amplitude data through the use of the gray-level co-occurrence matrix (GLCM). First introduced by Haralick et al. (1973), Reed and Hussong (1989) and Gao (2003) applied gray level co-occurrence matrix to seismic data in order to quantify seismic stratigraphic textures. Such texture attributes hold significant promise in quantifying geological features such as mass transport complexes, amalgamated channels, and dewatering features that exhibit a distinct lateral pattern beyond simple edges. Like seismic waveform classification (Coléou et al., 2003), and spectral components, GLCM attributes are amenable to subsequent clustering analysis using self-organizing and generative-topographic maps (Angelo et al., 2009; West et al., 20032; Gao, 2007; Wallet et al., 2009).

We begin by defining texture in terms of tactile sensation and amplitude variability using the GLCM. We then show how we generalize GLCM attributes typically applied to a photographic image or a seismic horizon slice to a 3D seismic volume and show how our GLCM attributes can be used to analyze the results using an SOM algorithm by projecting SOM prototype vectors onto a 2D color bar (Matos et al., 2009). Next, we apply our workflow on data over Oswego Formation containing thin channels and a chert reservoir for a 3D survey acquired over Osage Co., OK, USA. Finally, we conclude with a summary of advantages and limitations of this method.

Texture

Hall-Beyer (2007) defines texture as “an everyday term relating to touch that includes such concepts as rough, silky, and bumpy. When a texture is rough to the touch, the surface exhibits sharp differences in elevation within the space of your fingertip. In contrast, silky textures exhibit very small differences in elevation". Seismic textures work in an analogous manner with elevation replaced by amplitude, and the probing a finger by a rectangular or elliptical analysis window oriented along the local dip and azimuth of the structure.

The Gray Level Co-occurrence Matrix

The GLCM is a tabulation of how often different combinations of voxel amplitude/brightness values (gray levels) occur in an analysis window. Intuitively, we mentally apply texture analysis any time we view a shaded-relief time-structure map. We recognize piecewise smooth surfaces separated by discrete faults, tightly folded areas, and chaotic zones. Our method differs from others (West et al.,2002 and Gao, 2003, 2004, 2007, 2009), in two ways. First, our method is structure-oriented and can therefore be applied to unflattened 3D seismic volumes. Second, our goal is to compute textures sensitive to lateral changes rather than vertical changes in reflectivity. Given that the seismic wavelet modulates the reflection coefficients and hence the subsurface lithology, we think that measures such as spectral decomposition and dip convergence do an excellent job of measuring amplitude variability normal to a locally dipping plane. Instead, we use the vertical window to 'stack' these texture measures. Parallel to the local dip, we define a local analysis window. We also reformat the data from 32-bit data to $2N_L+1$ levels, with values from 1 to N_L correlating to troughs, N_L+1 to a zero-crossing, and from N_L+2 to $2N_L+1$to peaks. Figure 1 shows a quantization example when levels vary between 1 and 9, where values of 1-4 correspond to troughs, 5 to zero crossings, and 6-9 to peaks.

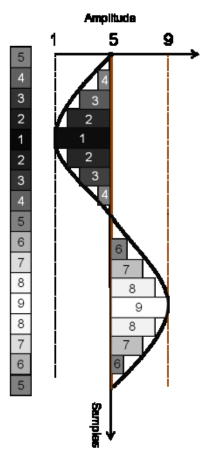

Fig. 1 - Quantization of a seismic trace using nine gray levels. Levels 1-4 represent troughs, 5 zero crossing, and 6-9 peaks. We find that quantization into 65 or 127 levels is sufficient for most seismic amplitude and attribute volumes. Coarser quantization with few levels results in clipped volumes that result in artificial homogeneous patches of data.

Next, we compute the GLCM, $(2N_L+1)$ by $(2N_L+1)$ matrix, within a $(2m_x+1)$ by $(2m_y+1)$ window along the k^{th} horizon slice:

$$P_{ij} = \sum_{p=-m_x}^{+m_x} \sum_{q=-m_y}^{+m_y} \delta(d_{p,q,k} - i)\delta(d_{p+\Delta p,q+\Delta q,k} - j) \qquad (1)$$

where i and j vary from 1 to $2N_L+1$, $d_{p,q,k}$ and $d_{p+\Delta p,q+\Delta q,k}$ are the integer-valued scaled seismic data at the (p,q) and $(p+\Delta p,q+\Delta q)$ CDP locations and the delta function, $\delta(\xi)=1$ if $\xi=0$ and 0 otherwise. We choose a suite of offsets Δp and Δq to represent repetitive patterns at angles of 0^o, 45^o, 90^o and135^o to the inline axis. We have found that scaling and quantizing our seismic amplitude, or any other desired attribute volume to integer values ranging between -32 and +32 (or $2N_L+1=65$) provides sufficient dynamic range yet manageable-sized matrices, **P**.

In summary, we need to define four parameters in constructing the GLCM:

- the quantization level of the image,
- the size of the moving window,
- the direction and distance of voxel pairs, and
- the statistics used as a texture attribute.

GLCM texture analysis workflow

Our 3D workflow is described by the flow chart shown in Figure 2. First, we precompute dip and azimuth at every seismic sample using one of the alternative 3D volumetric dip calculation algorithms (Randen et al. 2000; Barnes, 2000; Chopra and Marfurt, 2007; Fomel, 2008). Next, we extract data windows that are $(2m_x+1)$ by $(2m_y+1)$ traces wide by $(2K+1)$ time or depth samples thick along dip and azimuth for each and every output location. For each temporal slice k we compute the maximum of the absolute value

$$U_k = \underset{i,j}{MAX}(|u_{ijk}|); \quad -m_x \le i \le +m_x, -m_y \le j \le +m_y \qquad (2)$$

and then scale and quantize the data according to

$$d_{pqk} = NINT\left(\frac{u_{pqk}}{U_k} N_L\right) + N_L + 1 \qquad (3)$$

where the function NINT returns the nearest integer to its floating point argument, such that the resulting integer valued data fall within the range $-N_L \le d_{pqk} \le N_L$.

For each time or depth level k, we compute the $(2N_L+1)$ by$(2N_L+1)$ GLCM, **P**, using equation 1 followed by one or more attributes, g_k, using equations A-1 through A-8. A more robust GLCM attribute, G, is then computed from each level by

$$G = \sum_{k=-K}^{+K} w_k g_k , \qquad (4)$$

where

$$w_k = \frac{U_k}{\sum_{k=-K}^{+K} U_k} . \qquad (5)$$

To reduce low signal-to-noise problems, we use the real as well as imaginary components of the analytic trace to build the matrices P used to compute the attribute g_k in equation 4. Finally we cluster these attributes using self-organizing maps for further interpretational analysis.

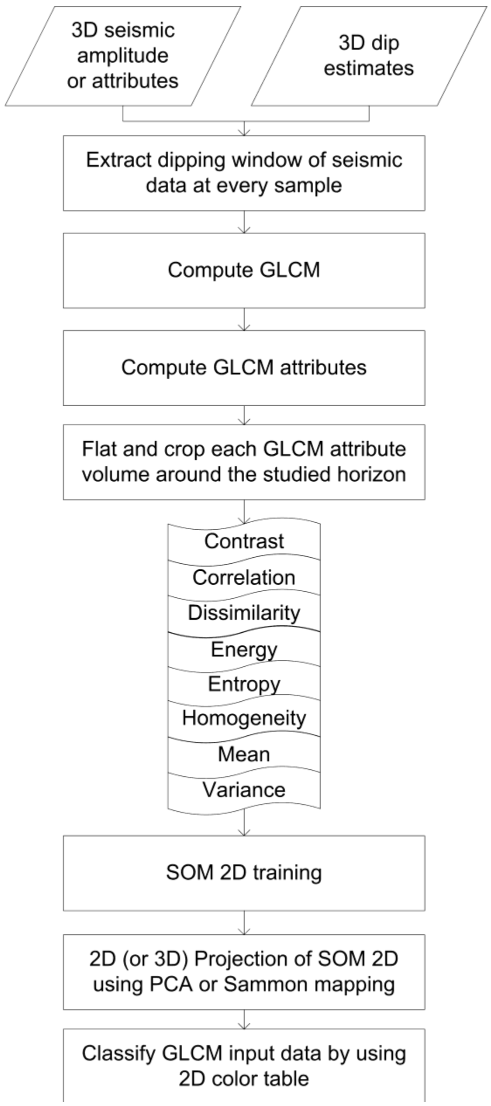

Figure 2. 3D GLCM computation workflow.

Self-organizing map (SOM)

Self-organizing maps, SOM, (Kohonen, 2001) and K-means clustering are the two most commonly used tools for non-supervised seismic facies analysis with SOM providing ordered clusters and are typically mapped against a 1D gradational color bar (Coléou et al., 2003). SOM is a special vector quantization method that represents multi-dimensional data by using a relatively low-dimension (1, 2, or 3) latent-space grid. Although the SOM has the same relatively high dimension of the input data, by construction SOM preserves the adjacent relationship among each SOM quantized vector (Matos et al., 2007). In this manner, SOM can be interpreted as a mapping of seismic attributes residing in *r*-dimension space onto a 1D, 2D, or 3D latent space that preserves the original topological structure of the seismic amplitude data (Wallet et al., 2009). In this paper we assume that the input variables to the SOM are the GLCM attributes while the resulting 2D SOM is mapped against a 2D color bar. The 2D color bar is created by applying the HSV color model to the projections of the SOM by using Principal Component Analysis or Sammon mapping onto a two dimensional plane (Matos et al., 2010).

Applications to 3D seismic data

The present study area is from Osage County, north-east Oklahoma, USA (Figure 3). It is bounded by the Ozark uplift to the east, the Nemaha uplift to the west, the Kansas state boundary to the north, and the Arkansas river to the southwest. Red Fork sandstone and Mississippian Limestone reservoirs from this area have been characterized by using GLCM attributes (Yenugu et al., 2010). In this paper, we applied SOM clustering technology associated with GLCM attributes to identify the Pennsylvanian channels and to characterize the Mississippian chert reservoir from the same area.

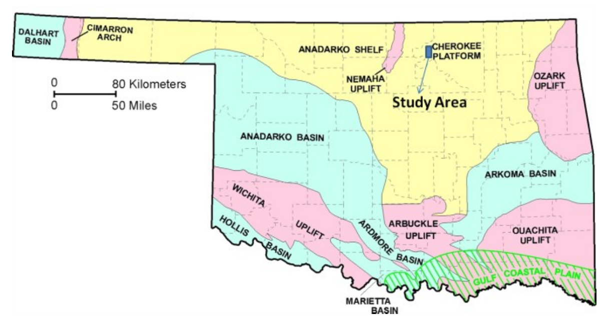

Fig. 3 - Map showing the geological provinces of Oklahoma. The study area is in Osage County, the Cherokee platform, northeast Oklahoma (Modified after Northcutt and Campbell, 1995).

First, we generated seven GLCM attributes from the 3D seismic data: contrast, energy, entropy, dissimilarity, homogeneity, mean, and variance. Then, we flattened each GLCM attribute volume around Oswego horizon and cropped them 10 samples above and 59 samples below Oswego, to make every trace with 70 samples (138 ms time interval). Figure 4 shows vertical slices along line AA' through GLCM flattened attributes. These seven GLCM cropped volumes were combined such that each voxel represents seven GLCM attributes. We, then, apply SOM and map the prototype vectors against a 2D color bar as shown in Figure 5b and described by Matos et al. (2009). The SOM classification results in a 3D volume with the same dimensions as a single GLCM attribute volume. Figure 5a shows the SOM vertical section along the inline AA' and Figure 5c shows the seismic amplitude section for the same inline. Both sections are flattened as the Oswego horizon.

Identification of Pennsylvanian channels

Stratigraphically, the top of the Pennsylvanian age is the Oswego limestone and the base is the Red Fork sandstone. The Verdigris sandstone, the Skinner sandstone and the Pink sandstones fall in between the Oswego and the Red Fork. The independent oil and gas operators do not show interest in targeting these channels since they cannot be identified through seismic. We used our SOM technique on GLCM attributes and scanned the slices from Oswego horizon. We observed two different meandering channels on the slice of sample no. 26, 30 ms below Oswego, (Figure 6b) and named them channel-A (white arrow) and channel-B (red arrow). The corresponding seismic phantom horizon is shown on Figure 6a. Scanning further into the Pennsylvanian formation, the channel-B disappeared, whereas channel-A appeared very clear meandering on the slice of sample no. 30, 38 ms below Oswego (Figure 6d). The corresponding seismic phantom horizon is shown on Figure 6c. Hence the SOM clustering technology applied on GLCM attributes brought out two distinctive Pennsylvanian meandering channels, which were not mapped before using 3D seismic data. Though Well-1 (Figure 7) was drilled through channel-A, no well log information was available to characterize this channel and verify the classification result.

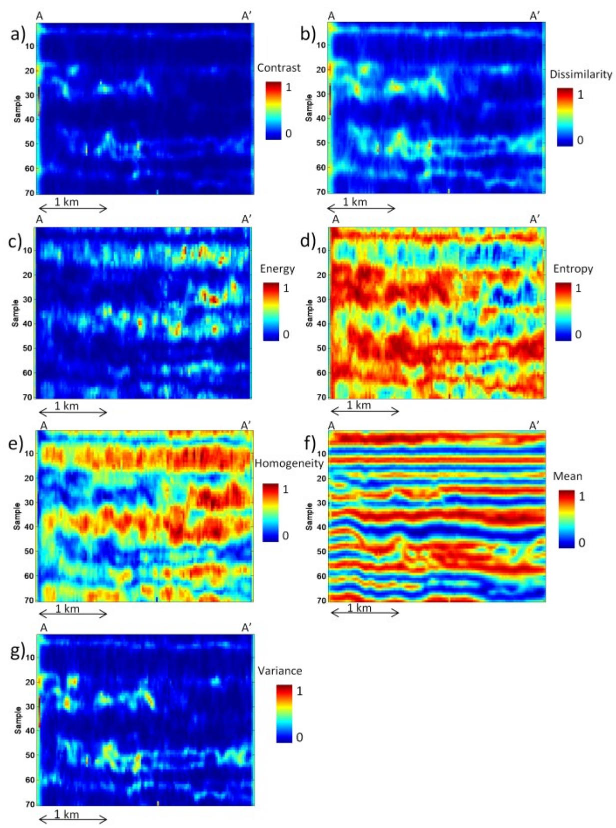

Fig. 4 - Vertical slices along line AA' through GLCM attributes: a) contrast; b) dissimilarity; c) energy; d) entropy; e) homogeneity; f) mean; and g) variance.. Location of line is shown Figures 12 and 13.

Characterization of the Mississippian chert reservoir

Chert is siliceous and composed of Silicon Dioxide (SiO_2). It represents an unconventional reservoir rock and is productive in West Texas, northern Oklahoma, south-central Kansas, California and Canada (Rogers and Longman, 2001). The Mississippian chert is a complex reservoir and is a significant oil and gas producer in the Mid-Continent. Chert is a non uniformly deposited rock with thickness, porosity, permeabilityand fluid saturation varying from well to well within the same field. Mapping these unconventional rocks on seismic is a big challenge for the interpreters. Seismic attributes like RMS amplitude and dominant frequency do not yield fruitful results for chert reservoir characterization. We applied ourSOM clustering technology of the GLCM attributes to characterize the unconventional cherty reservoir.

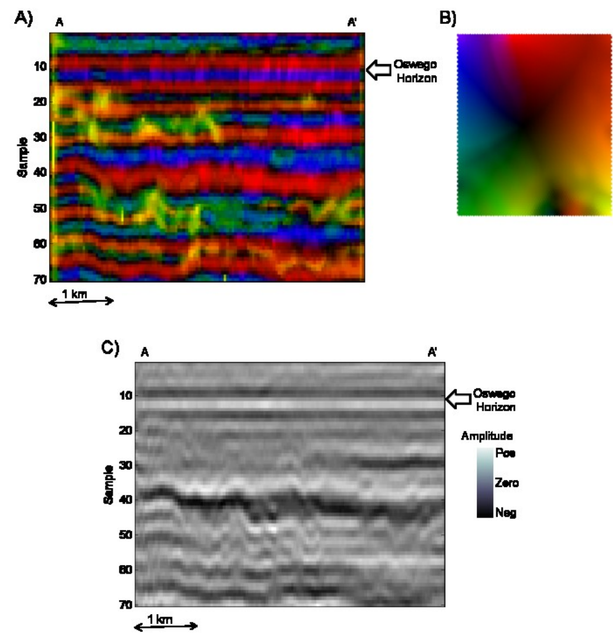

Fig. 5 - Vertical slices along line AA' through (a) SOM clusters computed from volumetric GLCM attributes, its (b) SOM 2d colorbar, and (c) seismic amplitude. Location of line is shown Figures 6 and 7.

A horizon slice (Figure 7) is extracted within Mississippian chert reservoir zone. We identified three different facies based on the SOM map. Facies-I correspond to deep blue to blue green color, Facies-II correspond to light to deep red color and Facies-III correspond to light to medium green color on the map. These facies indicate the distinctive nature of deposition of chert rocks. We tried to calibrate the facies maps with the available log and production data from the wells and observed that the Facies-I in Wells 1 and 2 are good producers of oil and gas with high porosities and permeability. The Well-3 which is drilled through Facies-II is a tight reservoir with less hydrocarbon saturation. No well was drilled through Facies-III to characterize them based on this map. The facies map generated on GLCM attributes using SOM clustering technology has been used to understand the heterogeneity in terms of reservoir facies, porosities and saturation within the same chert reservoir formation. Thus the SOM clustering technology has been used to understand the distinctive reservoir properties of chert reservoir.

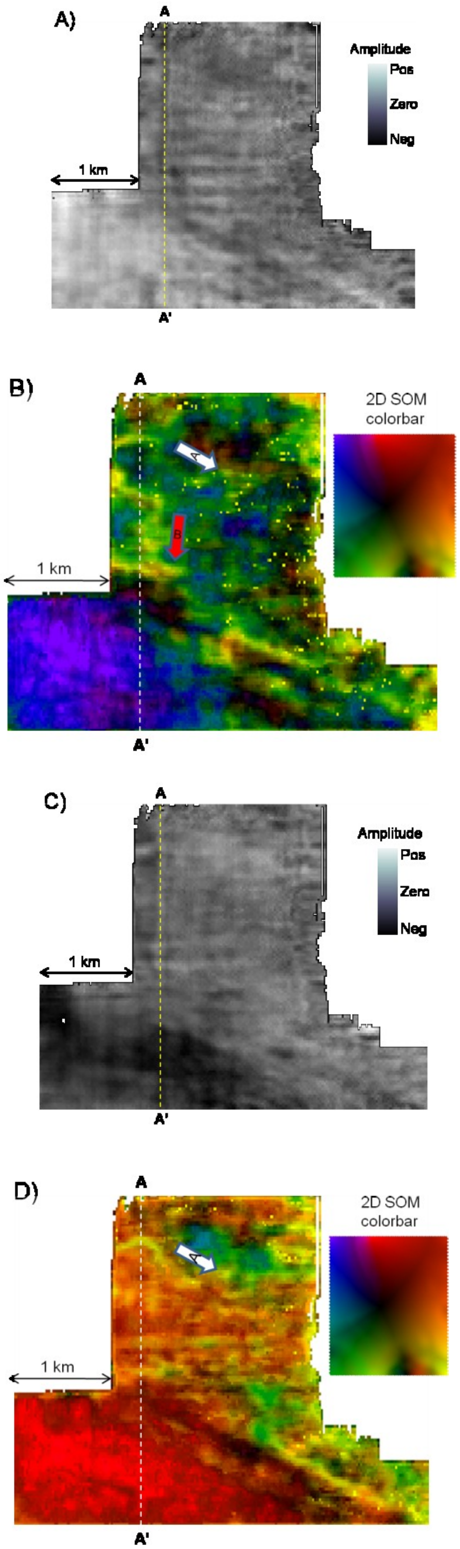

Fig. 6 - (a) Seismic amplitude phantom horizon 30ms below Oswego horizon within Pennsylvanian; (b) SOM horizon slice 30ms below Oswego horizon. SOM 2D Color bar is shown on the right; (c) Seismic amplitude phantom horizon 38ms below Oswego horizon (d) SOM horizon slice 38ms below Oswego horizon. SOM 2D Color bar is shown on the right.

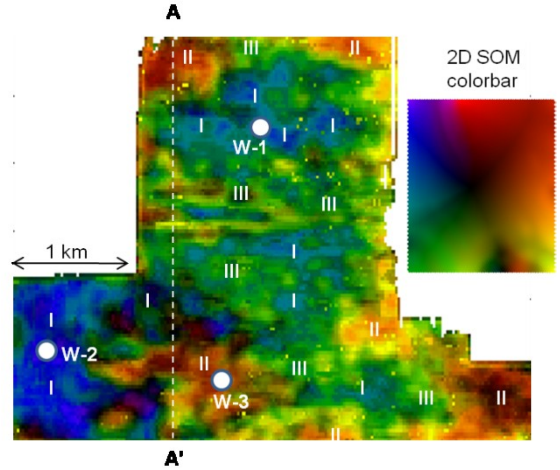

Fig. 7 - Horizon slice within chert reservoir through the SOM clusters computed from GLCM attributes. SOM 2D Color bar is shown on the top right. Roman numerals I, II, III correlate to good porous, tight and unknown facies respectively.

Conclusions

Traditional 2D seismic stratigraphy is based on a human interpreter identifying of subtle textures, such as onlap, offlap, unconformities, hummocky clinoforms, and parallelism. With the aid of volumetric attributes, 3D seismic geomorphology extends these concepts to volumetric data. While GLCM technology is commonly applied in remote sensing applications, it has not yet been widely accepted by the seismic interpreters community. We believe we have addressed several of the drawbacks that have caused difficulties in the past. First, we compute all our GLCMs along structural dip, thereby minimizing computational artifacts. Second, we perform our analysis on a 16-node processor, thereby reducing the relatively slow run times. Third, we avoid low-signal-to-noise issues by computing GLCM attributes from the analytic trace (separately using both real and imaginary parts) and stacking the results using a ±10 ms (11 slices) vertical analysis window using weights proportional to the maximum absolute amplitude of each slice. The GLCM attributes are less physical and therefore less-easily interpretable than more popular attributes like RMS amplitude, coherence, and curvature. For this reason, we combine our GLCM attributes using an efficient SOM clustering algorithm and plot the results against a 2D color bar, thereby minimizing the number of attribute volumes that need to be visualized and interpreted in a workstation.

The strength of our algorithm is also its limitation. By construction, we have avoided the important onlap, offlap, concordance, and hummocky clinoform patterns analyzed by workers using 2D vertical slices such as Ruffo et al. (2007). For this reason, a more robust interpretation workflow should include attribute sensitive to both lateral texture patterns (such as described in this paper) and vertical texture patterns (such as measured by spectral components). In summary, we believe that texture attributes hold significant promise in quantifying geological features such as mass transport complexes, amalgamated channels, and dewatering features that exhibit a distinct lateral pattern beyond simple edges. We also believe that our technique will be useful not only for delineation of reservoirs (Pennsylvanian channels), but also for more quantification of reservoir parameters (Mississippian chert) such as porosity, fluid saturation and pressure differences as used previously by Yenugu et al (2010) and Chopra and Alexeev (2006).

Acknowledgements

Thanks to the Spyglass Energy Group, Tulsa for providing a license to the seismic data volume used in this paper. Thanks also to the industry sponsors of the OU Attribute-Assisted Seismic Processing and Interpretation (AASPI) consortium.

References

Angelo, M. S., M. C. Matos and K. J. Marfurt, 2009, Seismic texture segmentation and clustering analysis to delineate reservoir geometry: 79th Annual International Meeting of the SEG, Expanded Abstracts, **28**, 1107-1111.

Barnes, A. E., 2000, Weighted average seismic attributes: Geophysics, **65**, 275–285.

Chopra, S., and V. Alexeev, 2006, Applications of texture attribute analysis to 3D seismic data: The Leading Edge, **25**, 934–940.

Chopra, S. And K.J. Marfurt, 2007, Seismic Attributes for Prospect Identification and Reservoir Characterization: Society of Exploration Geophysicists.

Coléou,T., M. Poupon, and K. Azbel, 2003, Interpreter's Corner—Unsupervised seismic facies classification: A review and comparison of techniques and implementation: The Leading Edge, **22**, 942–953.

Fomel, S., 2008, Predictive painting of 3D seismic volumes: 77th Annual International Meeting of the SEG, Expanded Abstracts, **27**, 864-868.

Gao, D., 2003, Volume texture extraction for 3D seismic visualization and interpretation: Geophysics, **68**, 141-146.

Gao, D., 2004, Texture model regression for effective feature discrimination: Application to seismic facies visualization and interpretation: Geophysics, **69**, 958-967.

Gao, D., 2007, Application of three-dimensional seismic texture analysis with special reference to deep-marine facies discrimination and interpretation: An example from offshore Angola, West Africa: AAPG Bulletin, **91,** 1665-1683.

Gao, D., 2009, 3D seismic volume visualization and interpretation: An integrated workflow with case studies: Geophysics, **74,** W1–W12.

Hall-Beyer, M. 2007, The GLCM Tutorial, version 2.10, http://www.fp.ucalgary.ca/mhallbey/tutorial.htm, accessed March 7, 2009.

Haralick, R. M., K. Shanmugam, and I. Dinstein, 1973, Textural features for image classification: Institute of Electrical and Electronics Engineers Transactions on Systems, Man, and Cybernetics, **SMC-3**, 610–621.

Kohonen, T., 2001, Self-organizing maps, 3rd ed.: Springer-Verlag.

Love, P. L. and M. Simaan, 1984, Segmentation of stacked seismic data by the classification of image texture: 64th Annual International Meeting of the SEG, Expanded Abstracts, **3**, 480-482.

Matos, M. C., K. J. Marfurt and P. R. S. Johann, 2010, Seismic interpretation of self-organizing maps using 2d color displays: Brazilian Journal of Geophysics, **28**, 631-642.

Matos, M.C., P.L.M Osório, and P.R.S. Johann, 2007, Unsupervised seismic facies analysis using wavelet transform and self-organizing maps: Geophysics, **72**, P9–P21.

Northcutt, R.A. and J.A. Campbell, 1995, Geologic provinces of Oklahoma:AAPG Mid-Continent Section Meeting.

Randen, T., E. Monsen, C. Signer, A. Abrahamsen, J.-O. Hansen, T. Saeter, and J. Schlaf, 2000, Three-dimensional texture attributes for seismic data analysis: 70th Annual International Meeting of the SEG, Expanded Abstracts, **19**, 668-671.

Reed, T. B., and D. Hussong, 1989, Digital image processing techniques for enhancement and classification of SeaMARC II side scan sonar imagery: Journal of Geophysical Research, **94**, 7469-7490.

Rogers, J.P., and Longman, M.W., 2001, An Introduction to chert reservoirs of North America: AAPG Bulletin, **85**, 1-5.

Ruffo, P., A. Corradi, A. Corrao, and C. Antonio Corrao, Claudio Visentin, 2007, 3D hydrocarbon migration in alternate sand-shale environment through percolation technique, AAPG Search and Discover Article #90066©2007 AAPG Hedberg Conference, The Hague, The Netherlands.

Wallet, B. C., M. Matos, J. T. Kwiatkowski, and Y. Suarez, 2009, Latent Space Modeling of Seismic Data: An Overview, The Leading Edge, **29**, 1454-1459.

West, B., S. May, J. E. Eastwood, and C. Rossen, 2002, Interactive seismic facies classification using textural and neural networks: The Leading Edge, **21**, 1042-1049.

Yenugu, M., K.J. Marfurt, and S. Matson, 2010, Seismic texture analysis for reservoir prediction and characterization: The Leading Edge, **29**, 1116-1121.